



Efficiency of updating the ionospheric models using total electron content at mid- and sub-auroral latitudes

Daria S. Kotova^{1,2} · Vladimir B. Ovodenko¹ · Yury V. Yasyukevich^{3,4} · Maxim V. Klimenko¹ · Konstantin G. Ratovsky³ · Anna A. Mylnikova³ · Elena S. Andreeva⁵ · Alexander E. Kozlovsky⁶ · Nina A. Korenkova¹ · Ivan A. Nesterov⁵ · Yulia S. Tumanova⁵

Received: 16 April 2019 / Accepted: 19 November 2019 / Published online: 11 December 2019
© Springer-Verlag GmbH Germany, part of Springer Nature 2019

Abstract

Describing the current ionospheric conditions is crucial to solving problems of radio communication, radar, and navigation. Techniques to update ionospheric models using current measurements found a wide application to improve the ionosphere description. We present the results of updating the NeQuick and IRI-Plas empirical ionosphere models using the slant total electron content observed by ground-based GPS/GLONASS receivers. The updating method is based on calculating the effective value of the solar activity index, which allows minimizing the discrepancy between the measured and the model-calculated slant TEC. We estimated the updating efficiency based on the *foF2* observational data obtained by ionosonde measurements. We calculated the data for 4 stations: Irkutsk, Norilsk, Kaliningrad, and Sodankylä. We analyzed 4 days in 2014: March 22, June 22, September 22, and December 18. We found that, in some cases, upon updating, the IRI-Plas underestimates the *foF2*, whereas NeQuick, on the contrary, overestimates it. We found a seasonal dependence of the updating efficiency of the ionosphere model using slant TEC. Possible causes of this dependence might be associated with the seasonal dependence of the correctness of model's reproduction of the latitude–longitude TEC distribution. In general, we found the low level of the updating efficiency of the *foF2* using slant TEC. This can be mainly explained by the fact that the models describe the electron density vertical profile and ionospheric slab thickness incorrectly.

Keywords GPS · GLONASS · Slant total electron content · Update empirical ionospheric models · Ionosonde measurements · High-orbit radio tomography

Electronic supplementary material The online version of this article (<https://doi.org/10.1007/s10291-019-0936-x>) contains supplementary material, which is available to authorized users.

✉ Daria S. Kotova
darshu@ya.ru

Vladimir B. Ovodenko
ovodenko@gmail.com

Yury V. Yasyukevich
yasukevich@iszf.irk.ru

Maxim V. Klimenko
maksim.klimenko@mail.ru

Konstantin G. Ratovsky
ratovsky@iszf.irk.ru

Anna A. Mylnikova
manna@mail.iszf.irk.ru

Elena S. Andreeva
es_andreeva@mail.ru

Alexander E. Kozlovsky
alexander.kozlovsky@oulu.fi

Nina A. Korenkova
ninakorala@gmail.com

Ivan A. Nesterov
nia2002@yandex.ru

Yulia S. Tumanova
88julia88@mail.ru

- ¹ West Department of Institute of Terrestrial Magnetism, Ionosphere, and Radiowave Propagation, Russian Academy of Sciences, Kaliningrad, Russia
- ² Department of Physics, University of Oslo, Oslo, Norway
- ³ Institute of Solar-Terrestrial Physics of Siberian Branch of Russian Academy of Sciences, Irkutsk, Russia
- ⁴ Irkutsk State University, Irkutsk, Russia
- ⁵ M.V. Lomonosov Moscow State University, Moscow, Russia
- ⁶ Sodankylä Geophysical Observatory, Sodankylä, Finland

Introduction

Determining the current ionospheric conditions is an important problem for high-frequency (HF) radio, radar, and navigation facilities to operate effectively. Zolesi and Cander (2014) noted several problems in providing the information for the ionospheric radio channel and a necessity for predicting ionospheric conditions. They also proposed some approaches to solve those problems. For applications, empirical ionospheric models are used as a rule. The models of such kind are climate based, and they cannot precisely describe the current ionospheric conditions (space weather), both under quiet and under disturbed conditions (Pignalberi et al. 2018). To improve the precision of the description of the ionosphere, one can use techniques of assimilating the data obtained by various observational facilities: ground- and space-based ionosondes, GNSS receivers, incoherent scatter radars, and others.

One of the best-known projects in data assimilation is the Ionosphere Real-Time Assimilative Model (IRTAM) (Galkin et al. 2012). The IRTAM assimilates real-time data of the ionosphere vertical sounding (VS) into the IRI empirical model in real time. VS ionosondes enable measuring the ionospheric characteristics of the F2 layer and below. These measurements allow one to adjust the basic parameters for the ionospheric model: F2 layer critical frequency (f_oF2) and the corresponding F2 layer peak height (h_mF2). Alternative techniques to estimate ionospheric conditions are rather important issues due to the relatively low density of ionosonde and due to the absorption of the vertical sounding signal during severe heliogeophysical events.

GNSS has been widely used to monitor the ionosphere (Hofmann-Wellenhof et al. 2008; Afraimovich et al. 2013). Many stations are deployed globally, they are efficient and inexpensive, easy to install and maintain. Another advantage is the possibility to measure the total electron content (TEC) at a high rate simultaneously in several directions for each navigation satellite. A disadvantage of using the TEC is that the latter is an integral value and involves no information on the shape of the electron density vertical profile. As a result, it is impossible to localize the disturbance region in space and to obtain the electron density at a certain altitude. The TEC data have been actively assimilated into empirical and first-principles ionospheric models (Khattatov et al. 2005; Komjathy et al. 1998; Hernandez-Pajares et al. 2002; Solomentsev et al. 2013). A significant advance in developing the global assimilation model by using various datasets, including those derived from GNSS, is implemented in the Global Assimilative Ionospheric Model (GAIM) (Wang et al. 2004) and USU-GAIM (Schunk et al. 2003) models.

Most of the updating methods for empirical models use effective indices of solar activity. Recently, Pignalberi

et al. (2017) have reviewed updating the IRI model using such indices. Komjathy and Langley (1996) studied the improvement of the IRI-95 by using vertical TEC maps. This method led to a 32.5% improvement in determining the TEC. Bilitza et al. (1997), while attempting to improve the TEC description for a satellite altimeter, used ionosonde data to calculate the regional and global ionospheric-effective solar indices. The index was selected so that the f_oF2 values in the IRI corresponded to the measured ones. The study showed that (a) the improvement is several percentages and (b) using regional indices led only to slight improvements.

Krankowski et al. (2007) used GPS observations to investigate a possibility to estimate the f_oF2 from TEC maps for the European region. The authors obtained good agreement between the recovered and the measured f_oF2 values for quiet and disturbed conditions. In this case, the root-mean-square f_oF2 error was 1.0–1.5 MHz for mid-latitude stations in October 2003, within a period of significant geomagnetic storms. Barabashov et al. (2006) studied the efficiency of the IRI updating to improve the precision of f_oF2 and the maximum usable frequency prediction. For this, they used the data of the vertical TEC, recalculated from the slant TEC. In general, the authors obtained some improvements for mid-latitude stations, but not for all the cases addressed. For example, for station Rome, there was an improvement for June upon updating, but, for September there was deterioration. Migoya-Oru e et al. (2015) assimilated vertical TEC from global maps into the IRI-2012 model. As a result of comparing f_oF2 observational and the model data, there was on average an improvement of 0.9 MHz for high solar activity. For low solar activity, the assimilation did not lead to any significant improvement.

Nava et al. (2005) achieved about 50% efficiency when correcting the NeQuick by means of vertical TEC maps by selecting an effective value for the Az index related to the F10.7 index. Later, Nava et al. (2006) studied possibilities of correcting the NeQuick model using slant TEC data from single- and multiple-GNSS receivers. The authors showed that the TEC description considerably improved when using the data from network of receivers. However, in terms of f_oF2 , using a network of GNSS stations did not exhibit an essential difference as compared to using data from a single station.

Maltseva (2018) showed that TEC may be used to calculate the critical frequency of the F2-layer. The observational median of the equivalent ionosphere thickness is a coefficient describing the synchronism between the TEC variation and the f_oF2 . Wijaya et al. (2017) proposed an f_oF2 computation method based on the vertical TEC data from one GNSS receiver without using the ionosphere model. The comparison between the f_oF2 obtained and the data from three ionosondes within periods of high and low solar

activities showed that the square-mean deviation for the $foF2$ discrepancy is within 0.6–1.4 MHz.

Yasyukevich et al. (2017) proposed various schemes to remove the ionospheric error of radio systems, based on the data from a single-GNSS station. Simultaneously, the TEC data nowcasting may also be used to provide a way that offers maximum utility for HF communication (Zolesi and Cander 2014; Zhukov et al. 2018). According to Zolesi and Cander (2014), one of the most important issues is how to define ionospheric prediction and forecasting in a way that offers maximum utility for guidance in practical radio communication work. Ovodenko et al. (2015) proposed a technique to update the parameters of the ionospheric model by means of the slant TEC data of a single receiver to improve the accuracy of the UHF radar. The authors estimated the efficiency of correcting the IRI-2007 model for 2 days of the spring equinox in 2014, both for estimating the radar errors and for recovering the $foF2$. In both cases, the model updating resulted in an increase in radar accuracy. With this, there was a diurnal variation in updating efficiency. Further application of the technique using slant TEC at a distance of about 200–400 km from the addressed ionosonde showed that its operation efficiency for $foF2$ correction might notably depend on the season (Kotova et al. 2018).

Thus, the issue of the efficiency of using GNSS data in terms of updating empirical ionospheric models has been actively developed recently but requires further studies. Our objective is to investigate the diurnal-seasonal dependency of the efficiency of updating empirical ionospheric models, viz. the possibility of defining the $foF2$ values upon updating the IRI-Plas and the NeQuick with the slant TEC data. The practical relevance of this research is assessing the use of slant TEC data to update $foF2$ values in near real time for operational planning of HF broadcast modes.

Data and methods

Lunt et al. (1999) and Klimenko et al. (2015) showed that the plasmasphere might contribute significantly to the total electron content: up to 20% at daytime and up to 50% at nighttime. Because the updating method uses the TEC data up to 20,000 km, the model used should take into account the plasmasphere contribution to the TEC. We selected two empirical models of the ionosphere: NeQuick (Hochegger et al. 2000) and IRI-Plas (Gulyaeva et al. 2002) that meet such a requirement. In the International reference ionosphere (IRI) model (Bilitza and Reinisch 2008), the height profile of plasma frequency is based on maps for critical frequencies and for the corresponding heights of the maxima of the ionospheric layers: $foF2$, $foF1$, and foE , $hmF2$, $hmF1$, and hmE . The set of coefficients calculated according to data from the

global network of VS ionosondes is used in the model. The plasmaspheric part in the IRI-Plas is empirically modeled in order to fit the IRI standard profile at 400–600 km (Gulyaeva et al. 2002). The electron density profile for the ionosphere and the plasmasphere in the NeQuick is described by Epstein half-layers with the half-thickness parameters determined empirically (Hochegger et al. 2000; Coisson et al. 2006). The values for the profile supporting points foE , $foF1$, $foF2$ and for the M3000 (F2) parameter are inferred by using the coefficients obtained from VS data. Thus, both models are based on observational data from the ionosonde network but differ in the formulas and in the coefficients used to describe the electron density in the ionosphere and in the plasmasphere. Both models, i.e., NeQuick and IRI-Plas, extrapolate the vertical topside electron density profile up to GPS and GLONASS orbit altitudes, although the models were developed and tested primarily with ionospheric data covering altitudes to about 3000 km. Indeed, more correctly, the distribution of electron density in the topside ionosphere and plasmasphere should be described along magnetic field-lines (not vertically) (Schunk and Nagy 2009.). A vertical extrapolation is a fairly simple solution, but it does not represent physics and nature. Some examples of model disadvantages concerning this issue were presented by Klimenko et al. (2015) and Cherniak and Zakharenkova (2016).

To update ionospheric models, we used the TEC data obtained with ground-based GNSS receivers. The GPS/GLONASS dual-frequency phase or of the pseudorange measurements enables the determination of the TEC along the satellite-receiver beam (Hofmann-Wellenhof et al. 2008). Following Yasyukevich et al. (2015), to obtain absolute slant TEC we used phase and pseudorange TEC combination with a special procedure to solve for differential code bias. The TayAbsTEC and tec-suite (www.gnss-lab.org) software was used for calculations.

The method to update the ionospheric model is based on minimizing the target function (TF), which is the sum of squares of residuals between the measured TEC_{OBS} and the model TEC_{MOD} values for each observed satellite. For our calculations, we select only the satellites with elevation angles greater than 45° in all azimuthal directions. The variable parameter is the solar activity index Rz12:

$$TF(Rz12) = \sum_i \Delta TEC_i^2$$

where $\Delta TEC_i = \Delta TEC_{OBS} - \Delta TEC_{MOD}(Rz12)$ and i is the TEC observation ordinal number of the total number of observations used for correcting at a specified instant. The $Rz12_{eff}$ effective value is the solar activity index at which the target function reaches its minimum. As initial condition, we used Rz12 predicted value for the respective month

and year. We accumulate the measurements of the absolute slant TEC over a 10-min interval. The middle of the interval epoch corresponds to the correction time. This enables elimination of random measurement errors and “abnormal” measurements in data.

To validate the obtained results before and after the updating procedure, we used the manually processed VS data at mid-latitudes (Irkutsk, Kaliningrad) and high-latitudes (Sodankylä, Norilsk). Ionosondes enable one to obtain the information on the critical frequency, as well as on the height of the maximum for various ionospheric layers. The selected VS stations are located near ground-based GNSS receivers, whose data we used to update the models. The stations Norilsk and Irkutsk are equipped with the DPS-4 ionosonde, the station Kaliningrad provides the data from the PARUS-A ionosonde, and, in Sodankylä, the observations are taken by the “Alpha-Wolf” ionosonde (Enell et al. 2016).

Data analysis and results

For the analysis, we selected four geomagnetically quiet days in 2014: spring (March 22) and autumn (September 22) equinox periods, summer (June 22) and winter (December 18) solstice periods. December 18 was selected instead of December 22, because, on the latter day the geomagnetic activity increased. The days correspond to four seasons at medium solar activity. The updating method described in the previous paragraph has then been applied to four GNSS receivers: Sodankyla (67.37°N, 26.63°E) and Norilsk (67.37°N, 26.63°E) in the sub-auroral region and Irkutsk (52.17°N, 104.16°E) and Kaliningrad (54.4°N,

20.3°E) at mid-latitudes. At each location, the relevant $Rz12_{eff}$ has been computed by adapting the NeQuick and IRI-Plas to slant TEC data and the modeled $foF2$ values have been retrieved. Subsequently, the comparison between the modeled and the corresponding observed $foF2$ data has been carried out. The results are illustrated below.

Figure 1 shows deviations between modeled and observed values of the $F2$ -layer critical frequency and the slant TEC (STEC) at Sodankylä for NeQuick and IRI-Plas before and after updating procedure. We used data from satellites with elevation angles greater than 45° for STEC calculation. The results are presented only for March 22 and for September 22, 2014, because there were no GNSS data for June 22 and December 18, 2014. The Δ STEC decreased almost to zero which indicates a self-consistency of the data ingestion method. The Δ STEC reduction leads to a stable decrease in the $\Delta foF2$ upon correcting only for March 22, 2014. For September 22, 2014, the stable Δ STEC reduction upon correcting does not result in the $\Delta foF2$ decrease, except 16–18 UT for the IRI-Plas.

Figure 2 shows the deviation of the $foF2$ model values from the observed ones at Norilsk. Although we analyzed only magnetically quiet conditions in our study, there are data gaps in this sub-auroral station. They are related to signal absorption in the lower ionosphere. We may note a trend: upon updating the NeQuick, the modeled $foF2$ appeared greater than the measured one, and, inversely, upon updating the IRI-Plas, the retrieved $foF2$ appeared underestimated. This difference in the results is related to the differences in how the models describe the vertical electron density profile (peak parameters and slab thickness), particularly in the topside ionosphere and plasmasphere.

Fig. 1 Diurnal variations in the slant TEC deviations and $foF2$ at Sodankylä for March 22 and September 22, 2014, for the NeQuick (top row) and the IRI-Plas (bottom row). The dotted black line shows the model slant TEC deviation from the observations before updating, and the solid black line denotes the same after updating. The lines with hollow circles show the deviation of the modeled $foF2$ from the observed one before updating, and the lines with the filled circles show the same after updating

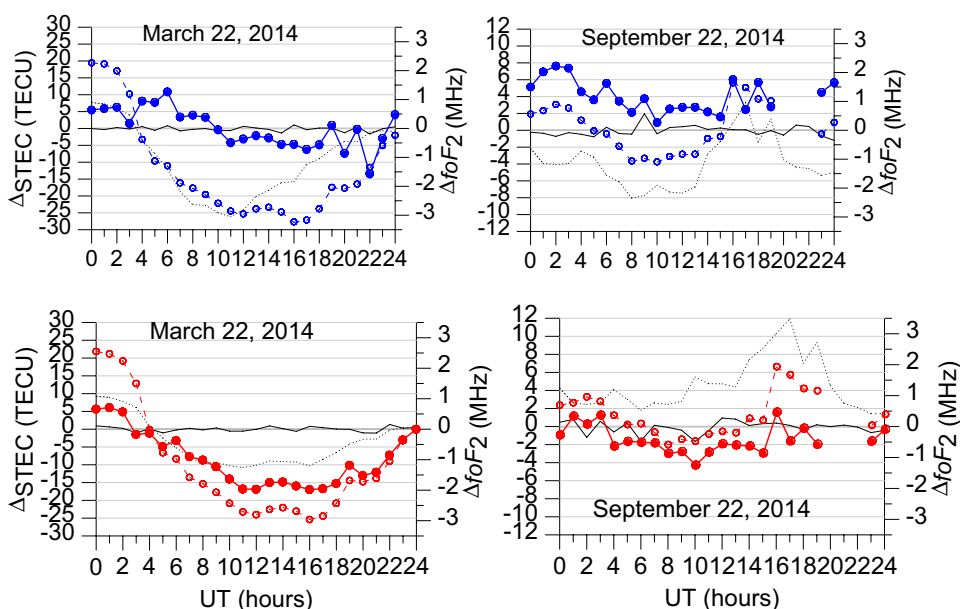


Fig. 2 Diurnal deviation of the $foF2$ model value from the observations at Norilsk for March 22, June 22, September 22 and for December 18, 2014. The dark blue color marks the results obtained by the NeQuick, and red color marks the results obtained by the IRI-Plas. Hollow circles and the dotted line show the results obtained before updating. Filled circles and the solid line show the results after updating

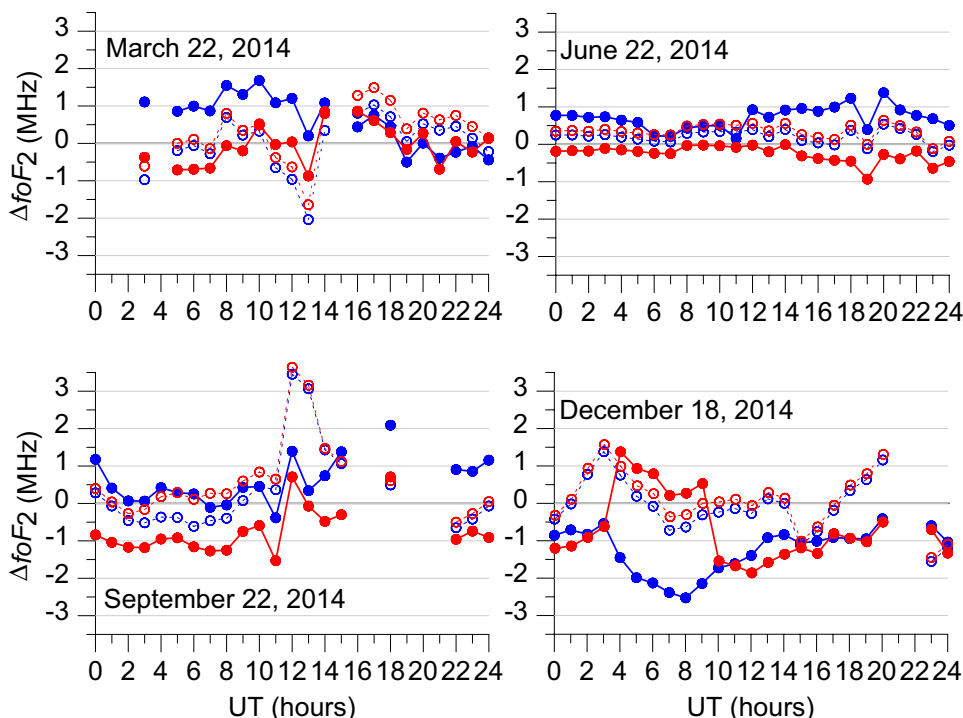


Fig. 3 Diurnal deviation of the $foF2$ modeled value from the observations at Irkutsk for March 22, June 22, September 22 and for December 18, 2014. Dark blue color denotes the results obtained by the NeQuick, and red color denotes the results from the IRI-Plas. Hollow circles and the dotted line show the results obtained before updating with the predicted Rz12. Filled circles and the solid line present the results after updating

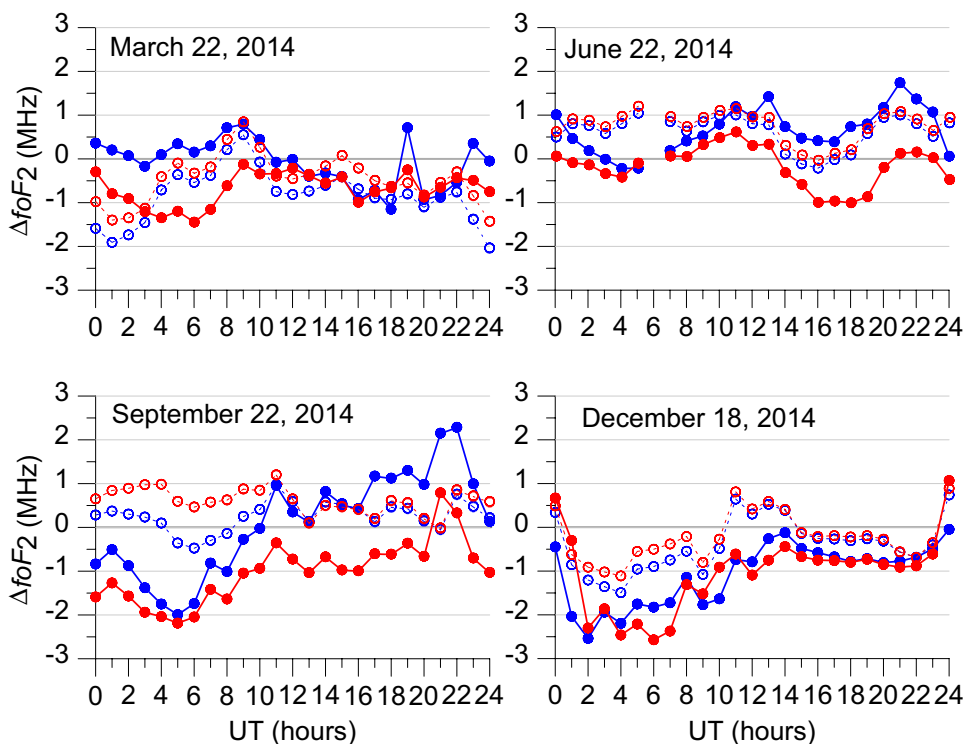


Figure 3 shows the diurnal variation of the $foF2$ deviations at Irkutsk. Practically, there are no data gaps in the VS data for the addressed quiet conditions, except for 6 UT on June 22, 2014. The update of the models was performed with the data obtained by the GNSS receiver located at Irkutsk. The $foF2$ model description after correcting the

NeQuick improved only for March 22, 2014, and, after correcting the IRI-Plas, it improved only for the summer solstice. On other days, both models described the $foF2$ diurnal variation with the Rz12 predicted value before updating better than after updating.

Fig. 4 Diurnal deviation of the $foF2$ model value from the observations at Kaliningrad for March 22, June 22, September 22, and for December 18, 2014. Dark blue color shows the results obtained by the NeQuick, and red color shows the results from the IRI-Plas. Hollow circles and the dotted line show the results obtained before correcting with a predicted Rz12. Filled circles and the solid line present the results after correcting

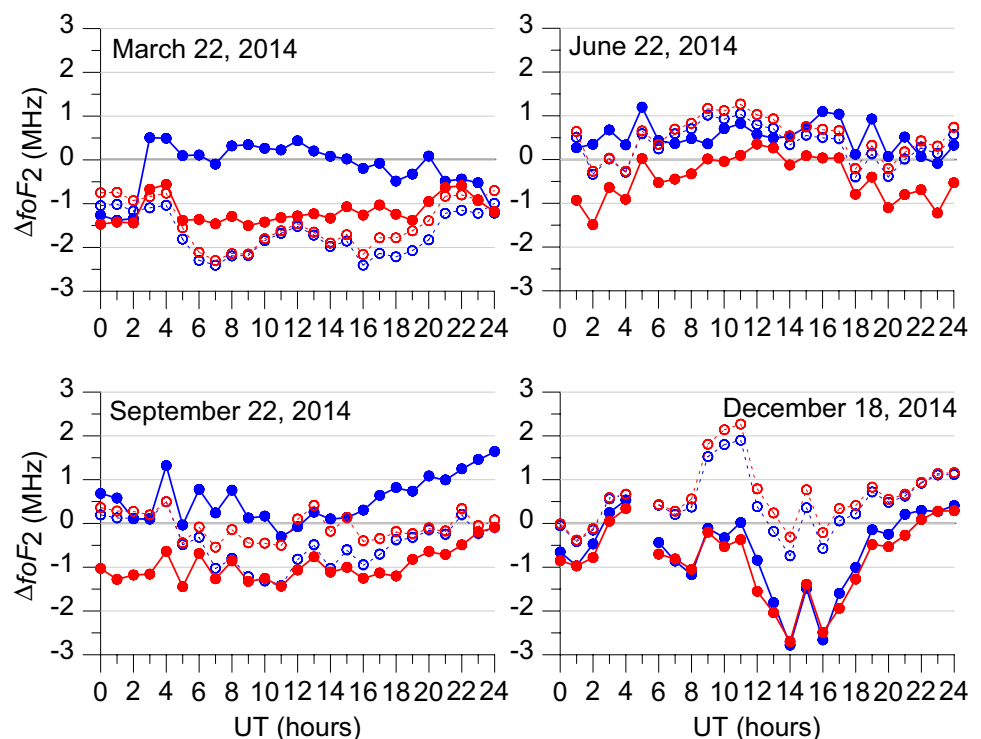


Figure 4 shows the results from the corrected model for Kaliningrad. We updated the ionospheric models by using a GNSS receiver located at Kaliningrad. From the figure, one can see that on March 22, 2014, updating both models in improving the $foF2$ model description. The best results were obtained for NeQuick, except those for night hours (00–02 UT). The updating led to increasing of an error of modeled $foF2$ for other days. For example, on June 22, 2014, the correction improved the model in the morning and daytime (07–13 UT), particularly in the IRI-Plas. However, during the remaining time, the $foF2$ without the model updating was closer to the measured values. For December 18, 2014, on the contrary, updating led to improvements in the evening hours (19–24 UT), whereas in the afternoon hours the updating impaired the $foF2$ reproduction in both models. For the autumn equinox (September 22, 2014), there is a good reproduction of the $foF2$ diurnal variation by the IRI-Plas without updating. Upon updating, the $foF2$ error increased. For the NeQuick, there was an improvement of the $foF2$ estimate for morning and afternoon hours (from 07 to 17 UT). Overestimating the results of the model calculations in the evening and night time led to an RMSE increase as compared with the RMSE when using the predicted Rz12 (without updating).

The root-mean-square diurnal averaged deviation of the $foF2$ model values from the observations without and with updating of the models for the four cases described above are presented in the supplementary material (Tables SM1–SM4).

The analysis of the results presented in Figs. 1, 2, 3, and 4 and Tables SM1–SM4 is given below. These data show that, on average, the maximal deviation of the model $foF2$ from the observed one was obtained for both models with the predicted Rz12 (without updating) during the spring equinox. The minimal deviation was obtained for the summer solstice. Updating the models led to improving the $foF2$ description in both models for March 22, 2014. The maximum deviation of the corrected $foF2$ values from the observed one was obtained for December 18, 2014. For that day, updating both models resulted in significant degradation of the results as compared with using the models without updating. The minimal error upon correcting the NeQuick was achieved for the spring equinox conditions. Upon updating the IRI-Plas, the above minimal error was achieved for the summer solstice. Updating the NeQuick parameters resulted in overestimating $foF2$ and updating the IRI-Plas, on the contrary, led to an $foF2$ underestimation.

Discussion

The principal conclusion is the following. There is a seasonal dependence for the efficiency of $foF2$ for updating the IRI-Plas and the NeQuick using STEC data by using the effective Rz12 parameter. The question is why the $foF2$ updating method is most effective at the spring equinox, and it is less effective at the solstice? We subsequently address

some aspects that may explain the $foF2$ errors after updating the models with the slant TEC data.

Using the TEC to correct the models may lead to an error due to a mismatch between the model and the observed electron density profile along the “satellite-receiver” ray-path. This error may be related to the problem of the model reproduction of the electron density latitude–longitude distribution in the ionosphere and in the plasmasphere of the earth. To investigate this assumption, we used the TEC distribution data obtained by high-orbit radio tomography (HORT). The HORT technique uses GNSS (GPS/GLONASS) radio-signals recorded by networks of ground-based receivers (IGS, UNAVCO, regional networks). The input data for the HORT are measurements of the carrier phases at the two operational frequencies. The problem of the unknown additive phase constant is solved through the phase-difference approach. The main feature of the HORT inverse problems from the GNSS data is their high dimensionality. A comparatively small angular velocity of GNSS satellite motion makes it necessary to consider the ionospheric temporal variability, i.e., to state the problem of four-dimensional (4D) tomography (three spatial coordinates and time) (Kunitsyn et al. 2010). The 4D problem makes input data incompleteness particularly essential: the satellite-receiver rays do not illuminate each point throughout the space but leave some domains blank and, thus, produce data gaps in the regions with few receivers. Also, the problem of non-uniqueness of the solution exists. Nesterov and Kunitsyn (2011) proposed an approach to overcome the non-uniqueness under the conditions of incomplete data. This approach is based on selecting the smoothest solution by minimizing a Sobolev norm for the required function. The HORT technique enables obtaining spatial–temporal (4D) electron density distribution in the ionosphere (both global and regional) with a spatial resolution of about 70–100 km, and with 30–60 min time increments in the regions with sufficiently dense networks of receiving stations. The HORT efficiency is corroborated by the results of numerous comparisons with ionosonde data (Kunitsyn et al. 2010, 2013).

For the addressed cases, we obtained HORT reconstructions of the electron density in the region of Europe based on the data from 121 stations of the IGS network. The range of geographic latitudes is -35° to 80° N, longitudes -10° to 60° . The step of a spatial–temporal grid for HORT reconstructions is about 0.7° in longitude, about 0.6° in latitude, 62 km in height, and 1 h in time. Based on the HORT reconstructions, we calculated the vertical TEC latitude–longitude distributions (TEC maps). For the same spatial grid, we simulated the TEC maps based on the IRI-Plas and on the NeQuick. The preliminary comparison of HORT TEC data with IRI-Plas and NeQuick model results obtained with and without taking into account updating procedure reveals that, in average, the model/data discrepancy decreases by

a factor of two after updating procedure. So this procedure allows to strongly improve slant and vertical TEC representation in the nearest neighborhood of the GNSS receivers. The same results were obtained by Nava et al. (2011). The supplementary materials (Figs. SM2–SM5) show the comparison between the model and the observed TEC maps for all the investigated cases. The qualitative analysis showed that the empirical models reproduce the TEC latitude–longitude structure better in March and worst in June. To quantitatively estimate the quality of the TEC latitude–longitude structure in the model, we calculated the Pearson correlation coefficients (PCC) of the modeled and observed TEC maps. The PCC was calculated for every hour of each of the 4 days. The correlation calculation was performed for the TEC spatial distribution functions: experimental, $F_{\text{exp}}(i)$; model IRI-Plas, $F_{\text{IRI}}(i)$; model NeQuick, $F_{\text{NeQuick}}(i)$. Here, i is put in the correspondence to the map cell number (“latitude”–“longitude” couple). Here, we did not use updating the models but would like to note that the updating procedure insignificantly influences the modeled TEC longitude–latitude structure. We addressed three longitude–latitude regions: (1) 35° – 80° N, -10° – 60° E; (2) 40° – 70° N, 0° – 40° E (the region around Kaliningrad with about 1500 km radius); (3) 50° – 80° N, -10° – 60° E (the region around Sodankylä with about 1500 km radius). According to the results presented in Tables SM5 and SM6 in the supplementary material, we can conclude that: (1) the best model-data agreement of the TEC spatial distribution is obtained for March 22, 2014, for the autumn equinox and winter solstice the correlation appeared lower, and the least correlation was obtained for the summer solstice; (2) the correlation coefficients for the mid-latitude region is, on average, higher than that of the high-latitude region; (3) the presented seasonal dependence of the models being able to reproduce the TEC latitude–longitude structure, correspondingly, may explain the seasonal dependence of the efficiency of the updating technique for $foF2$ determination over Kaliningrad and Sodankylä. Note that in the situation when modeled TEC is correct and modeled $foF2$ is not correct, the slab thickness problem may be one of the main issues that were shown by Migoya-Oru e et al. (2015) and Nava et al. (2011).

The joint data analysis showed that, in most of the addressed cases, the IRI-Plas (upon updating) underestimated the $foF2$ values relative to the ionosonde data, and the NeQuick, on the contrary, overestimated the $foF2$. Cherniak and Zakharenkova (2016), from the measurements of GPS signals onboard the GOCE and TerraSAR-X satellites, showed that, within 500–20,000 km heights, the IRI-Plas overestimates the TEC, whereas the NeQuick, on the contrary, underestimates it. Okoh et al. (2018) also drew a conclusion that the IRI-Plas usually overestimates the GNSS VTEC, whereas the NeQuick usually underestimates the latter. Gulyaeva and Gallagher (2007) detected

overestimating the plasmaspheric electron content from the IRI-Plas as compared with the Global Core Plasma Model-2000. Thus, overestimating the electron content in the upper ionosphere should result in underestimating the $foF2$, when updating the IRI-Plas. And, inversely, underestimating the electron content in the upper ionosphere should result in overestimating the $foF2$ when correcting the NeQuick. These facts are corroborated in the bulk of our results. Thus, we note the importance of the correct model description of the plasmasphere while updating the models using the slant TEC data by GNSS receivers.

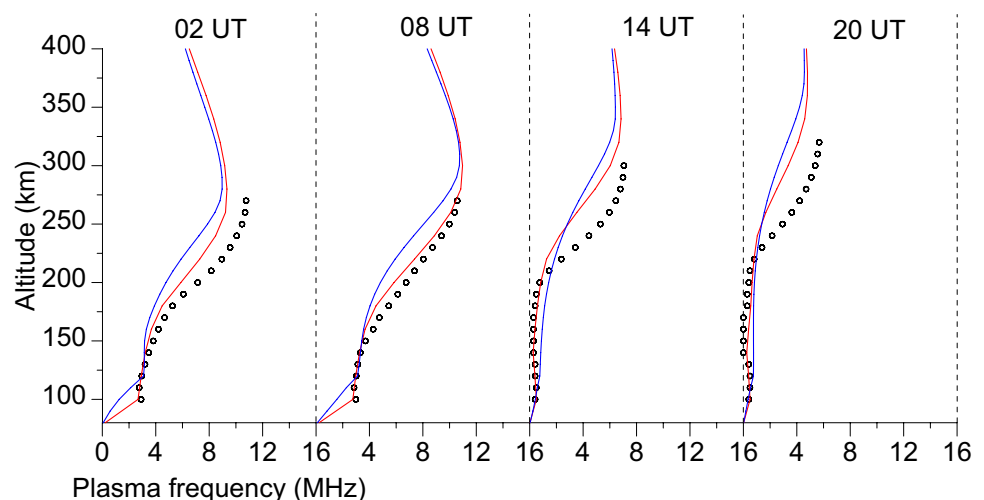
To test the correctness of the model's reproduction of ionospheric electron content, we used the recovered height profiles of the electron density from the ionosonde data at Irkutsk. We compared these profiles with the model height profiles of the electron density. Figure 5 shows the results for four instants of March 22, 2014. The plasma frequency profiles from observations were built as high as the maximum of the F2 electron density. Apparently, the F2 maximum height in the models is 30–40 km higher on average than the actually observed one. Both the shape and the half-thickness of the model ionospheric layer differ from the observed values. The vertical structure is described equally incorrectly both for the spring equinox conditions and for the other days addressed. We obtained a similar result for Norilsk. Thus, no common relation was revealed between the diurnal-seasonal dependency of the model correction efficiency and the reproduction of the models of the ionosphere height structure. However, one may confidently assert that it is the differences in the shape of the height profile that is one of the principal reasons for the inefficiency of the used updating technique to determine $foF2$.

Conclusion

We analyzed the efficiency of updating method of the IRI-Plas and NeQuick empirical models with the slant TEC data for the purpose of real-time $foF2$ updating. For the analysis, we used $foF2$ model data and $foF2$ measurements from VS stations located near ground-based GNSS receivers. The technique of updating the ionospheric models is based on minimizing the discrepancy between the measured and the modeled TEC by adjusting the effective index $Rz12$. The preliminary analysis reveals that in average, the model/data discrepancy decreases by a factor of two after updating procedure. So, this procedure is strongly effective for TEC improvement. Among the principal conclusions of our study, we may note the following:

1. There is a common seasonal dependence of the efficiency of updating the IRI-Plas and the NeQuick by using STEC for mid-latitude and sub-auroral ionosondes. Of the four magnetically quiet days addressed in 2014, our updating method operates best in terms of $foF2$ reproduction for equinox conditions and worst for the solstice conditions. Here, the models using a predicted $Rz12$ had the maximal deviation of the $foF2$ from the measured ones on March 22, 2014.
2. We studied a seasonal interrelation between the effectiveness of model updating and the correctness of the TEC latitude–longitude distribution by models. The IRI-Plas and the NeQuick, generally, reproduce the latitude–longitude structure of the TEC better during the equinox but worse during the solstice.
3. Our results indirectly corroborated that the IRI-Plas overestimates the electron content in the topside ionosphere and the plasmasphere, whereas the NeQuick underestimates the electron content. As a result, the IRI-

Fig. 5 Plasma frequency height profiles over Irkutsk at the vernal equinox day for 02:00, 08:00, 14:00, and 20:00 UT. The circles show the results of observational data from DPS-4, the red line presents the calculations with a predicted $Rz12$ by the IRI-Plas, and the dark blue line shows the latter by the NeQuick



Plas (upon updating) underestimates the $foF2$ values, whereas the NeQuick, on the contrary, overestimates them. Therefore, the efficiency of the $foF2$ reproduction using the algorithm for updating the IRI-Plas and the NeQuick varies. Hence, the result of correcting the ionospheric model by using slant TEC depends on the choice of climate-based model.

- Studying the height distribution of the electron content over Irkutsk showed that both models overestimate the observed F2-layer peak height by 30–40 km, on average. The models also describe the F2 half-thickness and the electron density profile shape incorrectly. It is one of the principal causes of the inefficient model updating with the slant total electron content for $foF2$ reproduction.

Acknowledgements We acknowledge Tamara Gulyaeva for the IRI-Plas code available via the IZMIRAN website (<ftp://izmiran.ru/pub/izmiran/SPIM/>), Telecommunications/ICT for Development (T/ICT4D) Laboratory of the Abdus Salam International Centre for Theoretical Physics, Trieste, Italy, for providing the NeQuick model code. We acknowledge IGS for GPS/GLONASS data (<ftp:// Garner.ucsd.edu/pub/rinex>). The SGO data of the $foF2$ are openly available at <http://www.sgo.fi/Data/Ionosonde/ionData.php> and at https://www.ukssd.c.ac.uk/wdccc/iivg_menu.html. The Kaliningrad, Irkutsk and Norilsk manually scaled ionosonde data and HORT data are openly available at https://github.com/darshu-dark/observation_data_for-GPS-Solutions-manuscript-of-Kotova-et-al. The data in Irkutsk region were recorded by using the *Angara* Multiaccess Center facilities at ISTP SB RAS (<http://ckp-rf.ru/ckp/3056/>) under budgetary funding from the Basic Research Program II.12. Data adaptation and checking of model correctness before and after updating procedure for stations at high-latitude were performed at financial support of the Russian Science Foundation (Grant 17-77-20009). The Irkutsk and Kaliningrad ionograms manual scaling, empirical model usage and model-data comparison was funded by the Russian Foundation for Basic Research (Grant № 18-55-52006). The work of E. Andreeva (radio tomography data processing and analysis) was supported by the Russian Foundation for Basic Research (Grant № 19-05-00941).

References

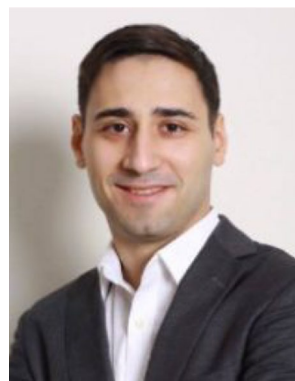
- Afraimovich EL et al (2013) Review of GPS/GLONASS studies of the ionospheric response to natural and anthropogenic processes and phenomena. *J Space Weather Space Clim* 3:A27. <https://doi.org/10.1051/swsc/2013049>
- Barabashov BG, Maltseva O, Pelevin O (2006) Near real time IRI correction by TEC-GPS data. *Adv Space Res* 37(5):978–982. <https://doi.org/10.1016/j.asr.2006.02.008>
- Bilitza D, Reinisch B (2008) International reference ionosphere 2007: improvements and new parameters. *Adv Space Res* 42(4):599–609. <https://doi.org/10.1016/j.asr.2007.07.048>
- Bilitza D, Bhardwaj S, Koblinsky C (1997) Improved IRI predictions for the GEOSAT time period. *Adv Space Res* 20(9):1755–1760. [https://doi.org/10.1016/S0273-1177\(97\)00585-1](https://doi.org/10.1016/S0273-1177(97)00585-1)
- Cherniak I, Zakharenkova I (2016) NeQuick and IRI-Plas model performance on topside electron content representation: spaceborne GPS measurements. *Radio Sci* 51(6):752–766. <https://doi.org/10.1002/2015RS005905>
- Coisson P, Radicella SM, Leitinger R, Nava B (2006) Topside electron density in IRI and NeQuick: features and limitations. *Adv Space Res* 37(5):937–942. <https://doi.org/10.1016/j.asr.2005.09.015>
- Enell C-F, Kozlovsky A, Turunen T, Ulich T, Väitalo S, Scotto C, Pezzopane M (2016) Comparison between manual scaling and Autoscala automatic scaling applied to Sodankylä Geophysical Observatory ionograms. *Geosci Instrum Method Data Syst* 5(1):53–64. <https://doi.org/10.5194/gi-5-53-2016>
- Galkin IA, Reinisch BW, Huang X, Bilitza D (2012) Assimilation of GIRO data into a real-time IRI. *Radio Sci* 47(4):RS0L07. <https://doi.org/10.1029/2011RS004952>
- Gulyaeva TL, Gallagher DL (2007) Comparison of two IRI electron-density plasmasphere extensions with GPS-TEC observations. *Adv Space Res* 39(5):744–749. <https://doi.org/10.1016/j.asr.2007.01.064>
- Gulyaeva TL, Huang X, Reinisch B (2002) Ionosphere–plasmasphere model software for ISO. *Acta Geod Geophys Hung* 37(2–3):143–152
- Hernandez-Pajares M, Juan J, Sanz J, Bilitza D (2002) Combining GPS measurements and IRI model values for space weather specification. *Adv Space Res* 29(6):949–958. [https://doi.org/10.1016/S0273-1177\(02\)00051-0](https://doi.org/10.1016/S0273-1177(02)00051-0)
- Hochegger G, Nava B, Radicella SM, Leitinger R (2000) A family of ionospheric models for different uses. *Phys Chem Earth Part C Solar Terr Planet Sci* 25(4):307–310. [https://doi.org/10.1016/S1464-1917\(00\)00022-2](https://doi.org/10.1016/S1464-1917(00)00022-2)
- Hofmann-Wellenhof B, Lichtenegger H, Wasle E (2008) GNSS—global navigation satellite systems. Springer, Wien. <https://doi.org/10.1007/978-3-211-73017-1>
- Karpachev AT, Klimenko MV, Klimenko VV, Pustovalova LV (2016) Empirical model of the main ionospheric trough for the nighttime winter conditions. *J Atmos Sol Terr Phys* 146:149–159. <https://doi.org/10.1016/j.jastp.2016.05.008>
- Khattatov B, Murphy M, Gnedin M, Sheffel J, Adams J, Cruickshank B, Yudin V, Fuller-rowell T, Retterer J (2005) Ionospheric nowcasting via assimilation of GPS measurements of ionospheric electron content in a global physics-based time-dependent model. *Q J R Meteor Soc* 131(613):3543–3559. <https://doi.org/10.1256/qj.05.96>
- Klimenko MV, Klimenko VV, Zakharenkova IE, Cherniak IV (2015) The global morphology of the plasmaspheric electron content during Northern winter 2009 based on GPS/COSMIC observation and GSM TIP model results. *Adv Space Res* 55(8):2077–2085. <https://doi.org/10.1016/j.asr.2014.06.027>
- Komjathy A, Langley R (1996) Improvement of a global ionospheric model to provide ionospheric range error corrections for single-frequency GPS users. In: Proceedings of ION AM 1996. Royal Sonesta Hotel, Cambridge, MA, June 19–21, pp 557–566
- Komjathy A, Langley R, Bilitza D (1998) Ingesting GPS-derived TEC data into the international reference ionosphere for single frequency radar altimeter ionospheric delay corrections. *Adv Space Res* 22(6):793–802. [https://doi.org/10.1016/S0273-1177\(98\)00100-8](https://doi.org/10.1016/S0273-1177(98)00100-8)
- Kotova DS, Ovodenko VB, Yasyukevich Y, Klimenko MV, Mylnikova AA, Kozlovsky AE, Gusakov AA (2018) Correction of IRI-Plas and NeQuick empirical ionospheric models at high latitudes using data from the remote receivers of global navigation satellite system signals. *Rus J Phys Chem B* 12(4):776–781. <https://doi.org/10.1134/S1990793118040127>
- Krankowski A, Shagimuratov II, Baran LW (2007) Mapping of $foF2$ over Europe based on GPS-derived TEC data. *Adv Space Res* 39(5):651–660. <https://doi.org/10.1016/j.asr.2006.09.034>
- Kunitsyn VE, Tereshchenko ED, Andreeva ES, Nesterov IA (2010) Satellite radio probing and radio tomography of the ionosphere. *Phys Usp* 53(5):523–528. <https://doi.org/10.3367/UFNe.0180.20105k.0548>

- Kunitsyn VE, Andreeva ES, Nesterov IA, Padokhin AM (2013) Ionospheric sounding and tomography by GNSS. In: Jin S (ed) Geodetic sciences—observations, modeling and applications. InTech, Rijeka, pp 223–252. <https://doi.org/10.5772/54589>
- Lunt N, Kersley L, Bailey G (1999) The influence of the protonosphere on GPS observations: model simulations. *Radio Sci* 34(3):725–732
- Maltseva OA (2018) Use of TEC to determine foF2: differences and similarities at high and low latitudes. In: ICTRS '18 proceedings of the seventh international conference on telecommunications and remote sensing. ACM, New York, pp 65–72. <https://doi.org/10.1145/3278161.3278172>
- Migoya-Oru e Y, Nava B, Radicella S, Alazo-Cuartas K (2015) GNSS derived TEC data ingestion into IRI 2012. *Adv Space Res* 55(8):1994–2002. <https://doi.org/10.1016/j.asr.2014.12.033>
- Nava B, Coisson P, Amarante GM, Azpiliculetta F, Radicella SM (2005) A model assisted ionospheric electron density reconstruction method based on vertical TEC data ingestion. *Ann Geophys* 48(2):313–320. <https://doi.org/10.4401/ag-3203>
- Nava B, Radicella SM, Leitinger R, Coisson P (2006) A near-real-time model-assisted ionosphere electron density retrieval method. *Radio Sci* 41(6):16. <https://doi.org/10.1029/2005RS003386>
- Nava B, Radicella SM, Azpilicuetta F (2011) Data ingestion into NeQuick 2. *Radio Sci* 46:RS0D17. <https://doi.org/10.1029/2010RS004635>
- Nesterov IA, Kunitsyn VE (2011) GNSS radio tomography of the ionosphere: the problem with essentially incomplete data. *Adv Space Res* 47(10):1789–1803. <https://doi.org/10.1016/j.asr.2010.11.034>
- Okoh D, Onwuneme S, Seemala G, Jin S, Rabiou B, Nava B, Uwamahoro J (2018) Assessment of the NeQuick-2 and IRI-Plas 2017 models using global and long-term GNSS measurements. *J Atmos Sol Terr Phys* 170:1–10. <https://doi.org/10.1016/j.jastp.2018.02.006>
- Ovodenko VB, Trekin VV, Korenkova NA, Klimenko MV (2015) Investigating range error compensation in UHF radar through IRI-2007 real-time updating: preliminary results. *Adv Space Res* 56(5):900–906. <https://doi.org/10.1016/j.asr.2015.05.017>
- Pignalberi A, Pezzopane M, Rizzi R, Galkin I (2017) Effective solar indices for ionospheric modeling: a review and a proposal for a real-time regional IRI. *Surv Geophys* 39(1):125–167. <https://doi.org/10.1007/s10712-017-9438-y>
- Pignalberi A, Pirotta M, Pezzopane M, Rizzi R (2018) Improvements and validation of the IRI UP method under moderate, strong, and severe geomagnetic storms. *Earth Planets Space* 70:180. <https://doi.org/10.1186/s40623-018-0952-z>
- Schunk RW, Nagy A (2009) *Ionospheres: physics, plasma physics and chemistry*, 2nd edn. Cambridge University Press, New York
- Schunk RW, Scherliess L, Sojka JJ (2003) Recent approaches to modeling ionospheric weather. *Adv Space Res* 31(4):819–828. [https://doi.org/10.1016/S0273-1177\(02\)00791-3](https://doi.org/10.1016/S0273-1177(02)00791-3)
- Solomentsev DV, Khattatov BV, Titov AA (2013) Three-dimensional assimilation model of the ionosphere for the European region. *Geomagn Aeron* 53(1):73–84. <https://doi.org/10.1134/S0016793212060114>
- Themens DR, Jayachandran PT, Galkin I, Hall C (2017) The empirical Canadian high Arctic ionospheric model (E-CHAIM): NmF2 and hmF2. *J Geophys Res Space Phys* 122(8):9015–9031. <https://doi.org/10.1002/2017JA024398>
- Wang C, Hajj G, Pi X, Rosen IG, Wilson B (2004) Development of the global assimilative ionospheric model. *Radio Sci* 39(1):RS1S06. <https://doi.org/10.1029/2002RS002854>
- Wijaya DD, Haralambous H, Oikonomou C, Kuntjoro W (2017) Determination of the ionospheric foF2 using a stand-alone GPS receiver. *J Geod* 91(9):1117–1133. <https://doi.org/10.1007/s00190-017-1013-2>
- Yasyukevich Y, Mylnikova AA, Kunitsyn VE, Padokhin AM (2015) Influence of GPS/GLONASS differential code biases on the determination accuracy of the absolute total electron content in the ionosphere. *Geomagn Aeron* 55(6):763–769. <https://doi.org/10.1134/S001679321506016X>
- Yasyukevich YuV, Ovodenko VB, Mylnikova AA, Zhivetiev IV, Vesnin AM, Edemskiy IK, Kotova DS (2017) GPS/GLONASS total electron content based methods for ionospheric error compensation for the radio communication systems. *Vestnik Povolzhsk State Technol Univ Ser Radio Eng Infocomm Syst* 2(34):19–31. <https://doi.org/10.15350/2306-2819.2017.2.19>
- Zhukov A, Sidorov D, Mylnikova A, Yasyukevich Yu (2018) Machine learning methodology for ionosphere total electron content nowcasting. *Int J Artif Intell* 16(1):144–157
- Zolesi B, Cander LR (2014) Introduction. In: *Ionospheric prediction and forecasting*. Springer geophysics. Springer, Berlin. https://doi.org/10.1007/978-3-642-38430-1_1

Publisher's Note Springer Nature remains neutral with regard to jurisdictional claims in published maps and institutional affiliations.



Daria S. Kotova received her Ph.D. degree in radio physics from the Institute of Solar-Terrestrial Physics SB RAS (ISTP SB RAS) in 2015. Now, she is a Senior Researcher at the WD IZMIRAN. She has 6 years of experience in ionospheric research and data processing. Her scientific interests include space weather impact on HF radio wave propagation and ionogram simulations of oblique sounding.



Vladimir B. Ovodenko received his Ph.D. degree in radar and navigation from the Radio Technical Institute in 2015. He works at the Pushkov Institute of Terrestrial Magnetism, Ionosphere and Radio Wave Propagation (West Department) of RAS as a researcher. His scientific interests include radar, transionospheric radiowave propagation, radar auroral backscatter, and meteors.



Yury V. Yasyukevich received his Ph.D. degree in radio physics from ISTP SB RAS in 2009. He works at the ISTP SB RAS as a leading researcher and at the ISU as an assistant professor. His scientific interests include monitoring and modeling based on GPS/GLONASS data; space weather impact on GPS/GLONASS; estimating the absolute total electron content; ionosphere anomalies. He is a PI of SIMuRG project (<http://simurg.iszf.irk.ru>).



Elena S. Andreeva received her Ph.D. in mathematical physics in 1992 from Lomonosov Moscow State University, Faculty of Physics, where she holds now an associate professor position. Her scientific interests mainly include physics of the upper atmosphere and ionosphere, GNSS remote sensing, satellite radio tomography of the ionosphere and near-space environment, space weather effects in the ionosphere–magnetosphere system.



Maxim V. Klimenko received B.S. in Physics in 2004 and a Ph.D. in 2008 at Kaliningrad State University. Now, he is a Senior Researcher at the WD IZMIRAN and Associate Editor of *Advances in Space Research*. He has over 10 years of experience in the development, modification, and application of numerical and empirical models of ionosphere and radio wave propagation.



Alexander E. Kozlovsky was graduated from the St. Petersburg (Leningrad) University in 1982. He was working as a researcher at the Plechenitsy Geophysical Observatory (Belarus) in 1982–1990, Polar Geophysical Institute (Apatity, Russia) in 1990–1998, and the Sodankyla Geophysical Observatory of the University of Oulu (Finland) since 1998. He is the author of more than 80 scientific papers on the ionospheric and magnetospheric physics.



Konstantin G. Ratovsky received Ph. D. in Physics and Mathematics from Institute of Solar-Terrestrial Physics SB RAS (ISTP SB RAS). Research experience includes Junior Researcher, Researcher, Senior Researcher, Leading Researcher, Head of Laboratory at ISTP SB RAS. Education and academic degree are as follows: graduate student at Irkutsk State University; as postgraduate student at ISTP SB RAS in November 1999 he defended his Ph.D. in Radiophysics.



Nina A. Korenkova received her B.S. degree in electronic computers in 1971 from Novosibirsk Electrotechnical Institute. She has been working as a Senior Researcher at the Magnetic Ionosphere Observatory “Ladushkin” of the WD IZMIRAN since 1974. She is an expert in the field of geomagnetic and ionospheric observations.



Anna A. Mylnikova received her Ph.D. degree in radio physics from the Institute of Solar-Terrestrial Physics in 2017. Her scientific interests include remote sensing of the ionosphere–upper atmosphere using signals of Global Navigational Satellite Systems; estimating the absolute vertical total electron content and differential code biases.



Ivan A. Nesterov was an associate professor of Lomonosov Moscow State University, Faculty of Physics (13.04.1972–16.03.2019). His scientific interests mainly included ill-posed problems of mathematical physics, GNSS radio tomography of the upper atmosphere and ionosphere, ionospheric adaptive modeling.



Yulia S. Tumanova received her M.S. degree in physics in 2011 from Lomonosov Moscow State University, Faculty of Physics, where she is currently completing a Ph.D. thesis. Her scientific interests include ionospheric remote sensing and radio tomography with GNSS, GNSS data processing, the morphology of ionosphere under various heliogeomagnetic conditions.